

Technical Notes

TECHNICAL NOTES are short manuscripts describing new developments or important results of a preliminary nature. These Notes should not exceed 2500 words (where a figure or table counts as 200 words). Following informal review by the Editors, they may be published within a few months of the date of receipt. Style requirements are the same as for regular contributions (see inside back cover).

Implications of Day Temperature for a High-Pressure-Turbine Blade's Low-Cycle-Fatigue Life Consumption

Muhammad Naeem*

National University of Sciences and Technology,
Rawalpindi 24090, Pakistan

DOI: 10.2514/1.32019

I. Introduction

HIGH-PERFORMANCE aircraft used in modern aviation, especially for military purposes, are complex in design and are required to operate under severe stresses and temperatures [1]. Thus, designer and users of these aircraft continually seek greater reliability, increased availability, enhanced performance, improved safety, and low life-cycle costs. Any extensions of the life expectations of aeroengines directly lower the life-cycle cost and depend upon the types of mission undertaken, operating conditions experienced, and rate of in-service engine deterioration.

Significant adverse effects of in-service aeroengine deterioration have been already established by earlier investigations [2–4]. However, as the result of a comprehensive literature review, it was realized that in addition to aeroengine deterioration, the condition of incoming airstream is also expected to have significant effects on an aeroengine's overall performance. In a country such as Pakistan, variation of day temperature over the year (i.e., from 0 to 50°C) significantly alters the condition of the incoming airstream. Any change in day temperature affects the quality of the incoming airstream for aeroengine operation as well as that of the air surrounding the air vehicles, thereby affecting the performance of both by altering atmospheric and aerodynamic characteristics [5]. As a result, an aeroengine will seek a different steady operating point, thereby resulting in a variation of the high-pressure spool speed (HS) for providing the same thrust to keep the aircraft's performance invariant. Any rise in the HS results in greater low-cycle-fatigue (LCF) damage for the hot-end components and thereby higher engine life-cycle costs. Possessing a better knowledge of the impacts of day temperature upon the LCF life consumption of an aeroengine's hot-end components helps the users to take wiser management decisions. Hence, this investigation was undertaken.

There are many components in an aeroengine, but its performance is highly sensitive to changes in only a few. Among these, the high-pressure turbine (HPT) blades are the most sensitive components, because they are subjected to both the highest rotating speeds and gas

temperatures [2], and so they were selected for the present investigation.

II. LCF Life-Consumption in Military Aeroengines

Considerable improvements in turbine-blade materials have allowed higher turbine entry temperatures (TETs), which in turn result in improved thrust and specific fuel consumption. However, achieving the highest possible TET requires an accurate knowledge of the turbine-blade temperature for the control and prolonging of engine life. The tradeoff of these increased temperatures is the increased risk of experiencing a blade failure. In addition to blade creep and oxidation, another possible mode of blade failure is pitting or cracking due to LCF [6]. In the 1960s, most critical components were limited by creep and stress rupture properties. Less than 1% of all rotating components were life-limited by LCF. However, today's designs find that well over 75% of these components are limited in life by LCF [7].

For a military fighter aircraft engine, LCF is the direct result of many throttle changes experienced. In addition to a wide range of missions flown by military aircraft, there can also be huge variations in the engine usage on what are nominally identical missions. For display aerobatics teams, the pilot of the lead aircraft will make fewer throttle movements than those pilots in the rest of the formation [8]. In addition, there is evidence of large variations in throttle handling that may occur between different pilots flying the same mission, even using the same aircraft type. May et al. [9], after studying several U.S. Air Force missions flown, concluded that different pilots made significantly different usages of the throttle while flying the same mission. Consequently, efforts to develop LCF life-usage monitoring have primarily been focused on military operations, to achieve economic lives in this highly demanding environment without compromising safety.

LCF damage of an aeroengine results from the application of varying loads. To determine these loads, it is necessary to relate them to measurable engine parameters. For example, the centrifugal stresses in a blade can be determined [10] via

$$S_i = S_{\text{ref}} \left[\frac{\Phi_i}{\Phi_{\text{ref}}} \right]^2 \quad (1)$$

An essential step in the prediction of the fatigue life is the reduction of a service strain or stress history to a series of cycles and half-cycles. This process is known as the cycle-counting method. The most widely used is the rain-flow, or Pagoda-roof, method first developed by Matsuishi and Endo [11] and then subsequently by others [12–14]. The same method was used for the present investigation.

The cycle-counting technique will transform the complex load history into a succession of stress ranges about a mean stress. The next stage is to calculate the actual LCF damage caused by each individual cycle. Two important methods are the stress-life and strain-life methods [15]. However, due to the concept of LCF as a high-strain fatigue, the strain-life method is generally considered to be more appropriate. First, the nominal centrifugal stress is calculated at each measured value of spool speed using Eq. (1). Then the local stress and strain at the notch for the first applied nominal stress is calculated using Neuber's rule [Eq. (2)] and the cyclic stress-strain curve [Eq. (3)], which may be combined to give Eq. (4) [16]:

Received 8 May 2007; revision received 3 November 2007; accepted for publication 11 February 2008. Copyright © 2008 by Muhammad Naeem. Published by the American Institute of Aeronautics and Astronautics, Inc., with permission. Copies of this paper may be made for personal or internal use, on condition that the copier pay the \$10.00 per-copy fee to the Copyright Clearance Center, Inc., 222 Rosewood Drive, Danvers, MA 01923; include the code 0748-4658/08 \$10.00 in correspondence with the CCC.

*Associate Professor, Deputy Head, Aerospace Engineering Department, College of Aeronautical Engineering, Pakistan Air Force Academy Risalpur; naeem1947@hotmail.com.

$$K_t^2 = \frac{\sigma \varepsilon}{S e'} \quad (2)$$

$$\varepsilon = \frac{\sigma}{E} + \left[\frac{\sigma}{K'} \right]^{\frac{1}{n}} \quad (3)$$

$$\left[\frac{\sigma^2}{E} \right] + \sigma \left[\frac{\sigma}{K'} \right]^{\frac{1}{n}} = \frac{(K_t S)^2}{E} \quad (4)$$

The local Delta stress is calculated by combining Eq. (2) with the hysteresis stress-strain rule of Eq. (5) to give Eq. (6) [16]:

$$\frac{\Delta \varepsilon}{2} = \frac{\Delta \sigma}{2E} + \left[\frac{\Delta \sigma}{2K'} \right]^{\frac{1}{n}} \quad (5)$$

$$\frac{(\Delta \sigma)^2}{2E} + \Delta \sigma \left[\frac{\Delta \sigma}{2K'} \right]^{\frac{1}{n}} = \frac{(K_t \Delta S)^2}{2E} \quad (6)$$

The local notch stress can be deduced by adding $\Delta \sigma$ to the value of σ at the origin of the hysteresis loop, and the local strain range $\Delta \varepsilon$ can be determined from Eq. (7):

$$\Delta \varepsilon = \frac{(K_t \Delta S)^2}{\Delta \sigma E} \quad (7)$$

The value of the local strain range is then inserted into the strain-life equation (8) to determine the cyclic life N_f :

$$\frac{\Delta \varepsilon}{2} = \frac{\Delta \varepsilon_e}{2} + \frac{\Delta \varepsilon_p}{2} = \frac{\sigma_f}{E} (2N_f)^b + \varepsilon_f (2N_f)^c \quad (8)$$

Equation (8) can be modified to account for the mean stress effects by including the mean stress σ_0 in the elastic-strain term [17]. This leads to

$$\frac{\Delta \varepsilon}{2} = \frac{(\sigma_f - \sigma_0)}{E} (2N_f)^b + \varepsilon_f (2N_f)^c \quad (9)$$

The final step is to sum the damage arising during each individual cycle. Several researchers have presented theoretical syntheses for predicting the cumulative damage. The most well-known is the Palmgren minor cumulative damage law [18], expressed as

$$\frac{n_f}{N_f} = \frac{n_1}{N_1} + \frac{n_2}{N_2} + \frac{n_3}{N_3} + \dots \quad (10)$$

When the value n_f/N_f , becomes unity, the component is considered to have failed. In reality, component failure occurs at ratios between 0.61 and 1.49 [19].

III. Computer Modeling and Simulations

Because of the enormous cost reductions and rapid results achieved relative to experimental/trial techniques, the use of validated computer-simulation techniques has attained recently the status of an advanced engineering procedure. Many scenarios can be simulated without incurring the major difficulties and expenses of preparing and testing engines. Hence, the implications of various factors (such as variations of deteriorations for the aeroengine, as a whole or for either of its major components, and changes in operating environment, such as day temperature, etc.) on engine performance can be studied and appreciated before they are encountered in service.

For this investigation, the performance of a McDonnell Douglas F-18 aircraft powered by two nominally identical F404-GE-400 aeroengines was assessed. The reason for selecting the F404 was twofold. First, the F404 engine is a typical new-technology engine

and, as such, the results of the investigation will be applicable to other similar new-generation engines. Second, sufficient relevant data were available [15,20].

In general, unlike those for civil aircraft, the mission profile (MP) for military aircraft can be relatively complex. However, for the purpose of the present analysis, the following (relatively simple) aircraft MP was assumed:

- 1) Short takeoff (TO) with reheat (RH), followed by climb to 6000 m while accelerating to Mach number $M = 0.6$ within 420 s.
- 2) Climb to 8000 m while accelerating to $M = 0.7$ in 250 s.
- 3) Climb to 10,500 m in 100 s followed by acceleration to $M = 1.0$ within 100 s.
- 4) Cruise until a preset time (1800 s from TO), followed by deceleration to $M = 0.95$ within 60 s.
- 5) Enhancement of engine power to 80%, attaining maximum Mach number, and then cruising at constant power (for a total time duration of 900 s), followed by acceleration/deceleration to $M = 0.85$ within 60 s.
- 6) Cruise for a set time period of 900 s, followed by cruise to cover a distance 500 km.
- 7) Acceleration as a result of RH for 60 s, followed by deceleration to $M = 0.85$ within 200 s by switching off the RH.
- 8) Descend to 8000 m within 300 s, followed by cruise toward the set target at 3000 km from the home base.
- 9) Descend to 4500 m while decelerating to $M = 0.5$ within 250 s, followed by loitering for 100 s.
- 10) Descend to land within 350 s, followed by landing approach, flare, touch down, ground roll, and, finally, switch off.

For the present investigation, the engine-performance simulation program NaeemPak, aircraft- and engine-performance simulation program NaeemPakA, and low-cycle-fatigue life-usage prediction program NaeemPakB have been used [15]. These programs were developed by the author while at Cranfield University. Details regarding atmospheric and aerodynamic characteristics, as well as the aircraft's performance throughout the MP (as described in [5,15]) and the strain-life technique [as described (very briefly) earlier], formed the basis for development of NaeemPakA and NaeemPakB, respectively. These programs were further enhanced and tailored to accomplish the present task.

NaeemPak is an updated version of the engine-performance simulation program Turbomatch [15]. Turbomatch has been used widely at Cranfield University for many years. Performance predictions from NaeemPakA using the simulation of an F-18 aircraft's behavior are reasonable, compared with published values [15,20]. A comprehensive study was discovered on LCF life consumption by Balderstone [10]. Because the method adapted for NaeemPakB was also principally taken from the same study, it was therefore decided to use this study for validation purposes. The final results achieved showed extremely close agreement with the case study. Based on the comparison of results with the case study and the cross-checking of all program submodels against hand calculations, it is considered that the model is sufficiently accurate at achieving a level of accuracy appropriate to the aims of the model, which were to be simple and generic, rather than definitive and special to type. The use of the model also confirmed the basic features affecting the HPT blade's life consumption, as detailed in the literature.

IV. Discussions and Analysis of Results

The prime factor responsible for any change in the HPT blade's LCF life consumption is the variation in the HS. A higher HS results in greater LCF damage and thereby higher blade LCF life consumption. The variations in day temperature would require the engine(s) to run at different HS to meet the thrust requirement for achieving the same aircraft's performance. For the present investigation, day-temperature variations are expressed in terms of International Standard Atmosphere deviation (ID) (i.e., an ID of 0, -15, and 35 K for a standard day temperature of 15°C and day temperatures of 0 and 50°C, respectively).

A. Aeroengine Behavior

Any MP would always be a combination of altitude (alt), Mach number M , and engine-power setting. Therefore, before an overall analysis of a HPT blade's LCF life consumption, it was considered appropriate to first see how HS is affected by any variation in alt/Mach-number/ID/engine-power setting or any combination of these. All HS values are expressed as a percentage of their design point value. The results are analyzed in subsequent paragraphs.

Figures 1–4 illustrate HS at stipulated conditions with increasing alt, Mach number, ID, and TET, respectively. A critical analysis establishes a significant and clear variation trend of HS with varying alt, Mach number, ID, and TET. For example, with varying ID and an increase of alt/TET, the whole pattern drifts toward the right (i.e., in the direction of increasing ID), whereas with an increase in Mach number, the pattern drifts toward the left. The HS peak value attained increases slightly with an increase in alt/Mach number and increases significantly with an increase in TET levels. With varying Mach

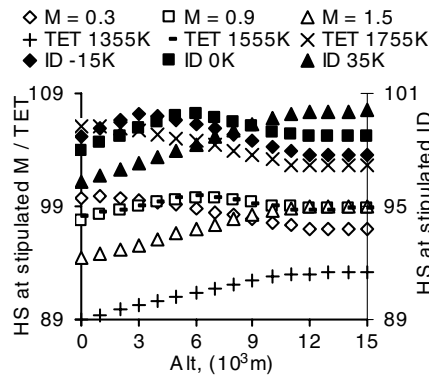


Fig. 1 HS at stipulated conditions with increasing altitude.

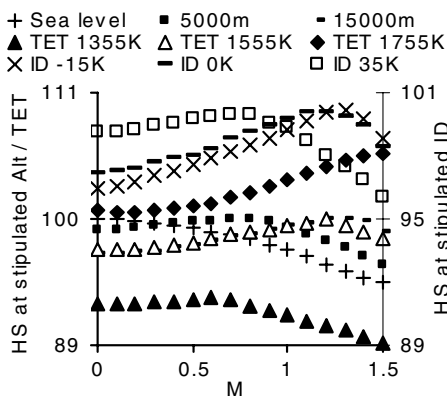


Fig. 2 HS at stipulated conditions with increasing Mach number.

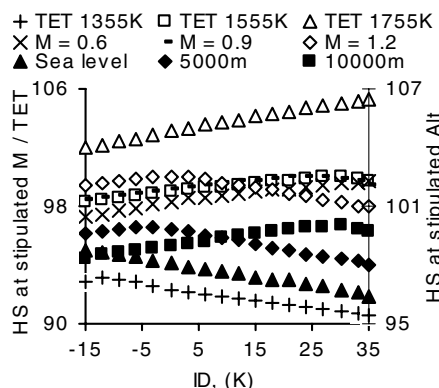


Fig. 3 HS at stipulated conditions with increasing ID.

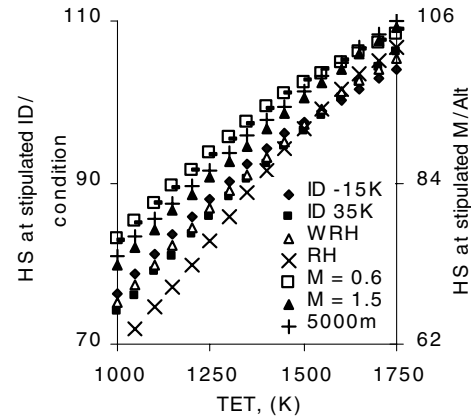


Fig. 4 HS at stipulated conditions with increasing TET.

number and with an increase of alt/TET, the whole pattern drifts toward the right (i.e., in the direction of increasing Mach number), whereas with an increase in ID, it drifts toward the left. The HS peak value attained increases slightly, decreases slightly, and increases significantly with an increase in alt, ID, and TET levels, respectively. For example, at 0-, 5000-, and 15,000-m alt, the HS peak value is 100, 100.02, and 100.09%, occurring at $M = 0.0, 0.8$, and 1.3 , respectively. At an ID of $-15, 0$, and 35 K, the HS peak value is 100.16, 100.09, and 99.95% occurring at $M = 1.3, 1.2$, and 0.8 , whereas at a TET of 1355, 1555, and 1755 K, the HS peak value is 93, 100.1, and 105.8%, occurring at $M = 0.6, 1.2$, and 1.5 , respectively.

At a given alt, Mach number, and ID, HS remains almost invariant for engines with RH and without (noted as WRH in Fig. 4). However, HS is lower for engines with reheat at TET levels lower than the design point, whereas it is lower for engines without reheat at TET levels higher than the design point. Also, for the same levels of alt and Mach number, the HS increases linearly with increasing ID for constant low-pressure spool speed (LS) and net thrust (NT), considered separately. The rise in HS is accompanied with rises in TET for both conditions. However, the rate of rise in HS and TET is significantly higher for constant NT than with that of a constant-LS condition.

B. Aeroengine–Aircraft Combination Behavior

While aircraft flies through the assumed mission profile (AMP), in addition to the behavior of fitted aeroengines in isolation, the behavior of the aeroengine–aircraft aerodynamic structure combination as a whole is of greater importance. During flight phases such as TO and combat RH, the aeroengine's peak performance plays the dominant role and aircraft performs according to the maximum available NT from engines. During some other flight phases (e.g., cruise at a specified alt and Mach number), the aircraft's aerodynamic characteristics play the dominant role and aeroengines are run at a power setting such that the NT available from engines balances the aircraft's drag. Therefore, the engine parameter of concern (i.e., HS) was also observed during some important flight phases and results are analyzed in subsequent sections.

Figures 5–8 illustrate HS during TO and RH, cruise (CRU) and acceleration (ACC), enhancement of power to 80%, followed by CRU at constant-power-setting flight phases for the stipulated ID and at different points on the MP with varying ID, respectively. A critical analysis establishes a significant variation (with differing variation trends) of HS during different flight phases as well as for different points on the MP with varying ID. For example, during the RH phase, HS increases with increasing RH time. At lower ID, HS increases with a slightly increasing rate, it increases almost linearly in the middle, and at higher ID, it increases with a slightly reducing rate. With RH, NT increases significantly and thereby results in acceleration of the aircraft. The behavior of the engine during RH is in line with the trend observed with increasing Mach number. At any given point on the MP, HS increases with increasing ID. For example, at the end of the TO phase (the most crucial phase, from

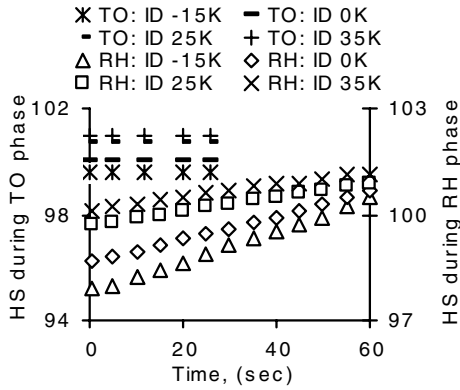


Fig. 5 HS during TO and RH phases at the stipulated ID with increasing flight time.

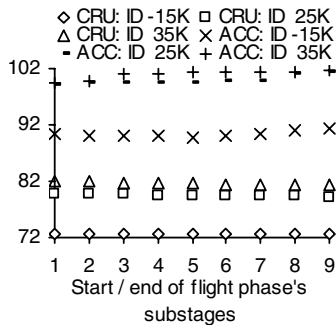


Fig. 6 HS during CRU/ACC flight phases.

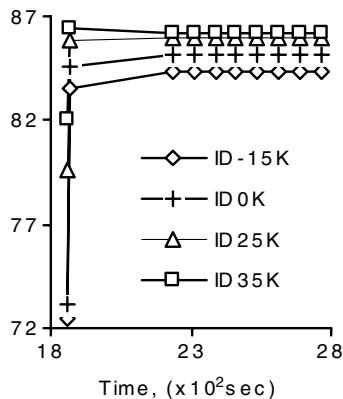


Fig. 7 HS at the stipulated ID, during enhancement of engine power to 80%, followed by cruise at constant power.

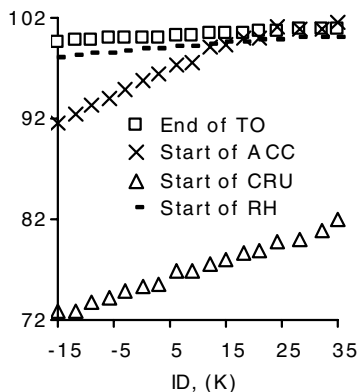


Fig. 8 HS at the start of RH/ACC/CRU and the end of the TO phase with increasing ID.

both safety and performance standpoints, in which the peak engine performance remains the dominant factor), HS is 99.6, 100, 100.7, and 101% at an ID of -15 , 0 , 25 , and 35 K, respectively. The HS rise with increasing ID is at the cost of rising TET. For example, the maximum TET attained during the TO phase rises to 1557, 1590, and 1605 K with an ID of 0 , 25 , and 35 K, respectively, compared with 1556 K with an ID of -15 K.

C. Representative Peacetime Training Mission Profiles for a Military Aircraft

Detail covered so far established differing variation trends of HS with varying alt, Mach number, and engine settings, thereby resulting in different trends for different flight phases and hence a different cumulative effect for the whole MP. Also, typical MPs for a military aircraft (dependent upon their role) vary significantly in terms of selection, combination, sequence (in the MP), and extent of different flight phases; each flight phase, in turn, varies significantly in terms of alt, Mach number, time duration, and required engine settings. Therefore, the exact effect of any variation in HS upon the overall LCF life consumption would vary with the type of MP. Hence, instead of restricting the present investigation to the AMP, it was considered appropriate to extend the analyses by considering representative peacetime training MPs, such as air superiority (AS), simple cruise (SC), low-level strike (LLS), and strategic bombing (SB) for a military aircraft [4].

D. HPT Blade's LCF Life Consumption

For the AMP, a blade's LCF life consumption increases significantly (but with differing rate of rise) with increasing ID. With clean engines, the blade's LCF life consumption at an ID of 25 and 35 K is 43.7 and 51.8% higher, respectively, than that at an ID of -15 K. The adverse effect becomes even more serious for engines suffering from a low-pressure compressor's fouling [3]. At an ID of 35 K, the blade's LCF life consumption for engines with 10% fouled compressors (FCmp in Fig. 9) increases by 95.8% (i.e., about a twofold increase), compared with clean engines at an ID of -15 K (see Fig. 9).

Among four representative MPs, AS is the severest in terms of a HPT blade's LCF life consumption. The blade's LCF life consumption at an ID of 35 K increases by 30.65%, compared with that at an ID of -15 K. In order of severity, the least severe is the SC MP. At an ID of 35 K, a blade's LCF life consumption for AS MP is 59, 43.65, and 19.54% higher than with SC, LLS, and SB MPs, respectively, whereas it is 102.33% higher than with a SC MP, but at an ID of -15 K.

With increasing ID, the trend and extent of rise in a blade's LCF life consumption vary significantly for different representative MPs. For a given MP type, it also varies with any change in nature/extent of flight segment(s), as well as with their interarrangement. For example, for AS MP, at an ID of 35 K, the HS is 1.4, 0.65, and 12% higher than with an ID of -15 K for TO, RH, and CRU to target-flight phases, respectively. The rise in HS is very small for TO and RH, compared with CRU; however, the point to note is that TO and RH are the two phases in which HS is already very high; therefore, a

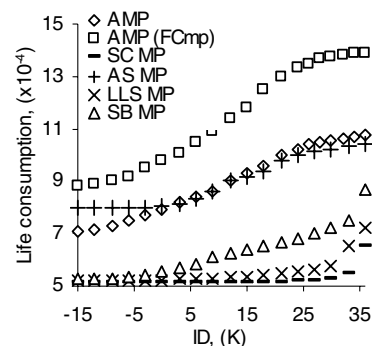


Fig. 9 HPT blade's LCF life consumption (for stipulated conditions) with increasing ID.

slight increase will have a remarkably adverse effect upon LCF life consumption.

The safe operational life of HPT blades for AS, SB, LLS, and SC MPs at an ID of 35 K reduces to 22.2, 40.3, 62.9, and 72.7%, compared with that for SC at an ID of -15 K (i.e., the blade's safe operational life reduces to about one-fifth for AS MP).

V. Conclusions

A computer simulation was used to explore the relative implications of day-temperature variations for a HPT blade's LCF life consumption in a turbofan engine. For the conditions assumed, the day-temperature variation has a significant adverse effect on a blade's LCF life consumption. The effect becomes even more significant for engines suffering from any deterioration, such as a low-pressure-compressor's fouling, and varies with the type of mission flown.

The results of such an investigation as the present for a variety of MPs under various operating conditions/engine deterioration levels will provide a wide database and can lead to managers taking wiser decisions. However, greater benefits will be achieved if the present analysis is considered as an integral part of a more comprehensive analysis, including aeroengine creep and thermal-fatigue-life uses, fuel-usage/weapon-carrying capability, aircraft-mission operational effectiveness, and life-cycle costs.

References

- [1] Devereux, B., and Singh, R., "Use of Computer Simulation Techniques to Assess Thrust Rating as a Means of Reducing Turbo-Jet Life Cycle Costs," International Gas-Turbine and Aero Engine Congress and Exposition, The Hague, Netherlands, American Society of Mechanical Engineers, Paper 94-GT-269, June 1994.
- [2] Naeem, M., Singh, R., and Probert, D., "Impacts of Aeroengine Deterioration on Military Aircraft Mission's Effectiveness," *The Aeronautical Journal*, Vol. 105, No. 1054, Dec. 2001, pp. 685–695.
- [3] Naeem, M., "Impacts of Low-Pressure (LP) Compressor's Deterioration Upon an Aeroengine's High-Pressure (HP) Turbine Blade's Life Consumption," *The Aeronautical Journal*, Vol. 110, No. 1106, Apr. 2006, pp. 227–238.
- [4] Naeem, M., "Impacts of Low-Pressure (LP) Compressor's Deterioration of a Turbofan Engine upon Fuel Usage of a Military Aircraft," *The Aeronautical Journal*, Vol. 112, No. 1127, Jan. 2008, pp. 33–45.
- [5] Daniel, P. Raymer, *Aircraft Design: A Conceptual Approach*, AIAA Education Series, AIAA, Washington, D.C., 1992.
- [6] Becker, W. J., Roby, R. J., O'Brien, W. F., and Bensing, G. K., "Dynamic Turbine Blade Temperature Measurements," *Journal of Propulsion and Power*, Vol. 10, No. 1, 1994, pp. 69–78.
- [7] Nicholas, T., Haritos, G. K., and Christoff, J. R., "Evaluation of Cumulative Damage Models for Fatigue Crack Growth in an Aircraft Engine Alloy," *Journal of Propulsion and Power*, Vol. 1, No. 2, 1985, pp. 131–136.
- [8] O'Connor, C. M., "Military Engine Condition Monitoring Systems: The UK Experience," AGARD Rept. CP-448, Neuilly-sur-Seine, France, 1988.
- [9] May, R. J., Jr., Chaffee, D. R., Stumbo, P. B., and Reitz, M. D., "Tactical Aircraft Engine Usage: A Statistical Study," AIAA, Paper 81-1652, Aug. 1981.
- [10] Balderstone, A. W., "A Generic Computer Model to Predict an Aeroengine's Low-Cycle Fatigue," M.Sc. Thesis, Cranfield Univ., Cranfield, England, U.K., 1996.
- [11] Matsuishi, M., and Endo, T., "Fatigue of Metals Subjected to Varying Stress," Society of Mechanical Engineers Conference, Fukuoka, Japan, Mar. 1968.
- [12] Dowling, N. E., "Fatigue Failure Predictions for Complicated Stress–Strain Histories," *Journal of Materials*, Vol. 7, No. 1, Mar. 1972, pp. 71–87.
- [13] Downing, S. D., and Socie, D. F., "Simple Rainflow Counting Algorithms," *International Journal of Fatigue*, Vol. 4, No. 1, Jan. 1982, pp. 31–40.
doi:10.1016/0142-1123(82)90018-4
- [14] Rychlik, I., "A New Definition of the Rainflow Cycle Counting Method," *International Journal of Fatigue*, Vol. 9, No. 2, Apr. 1987, pp. 119–121.
doi:10.1016/0142-1123(87)90054-5
- [15] Naeem, M., "Implications of Aeroengine Deterioration for a Military Aircraft's Performance," Ph D. Thesis, Cranfield Univ., Cranfield, England, U.K., 1999.
- [16] "Fatigue-Life Estimation Under Variable-Amplitude Loading Using Cumulative Damage Calculations," *Fatigue-Endurance Data Contents*, Vol. 2, Card No. ESDU 95006, IHS ESDU International, London, Sept. 1995.
- [17] James, A. G., "Fatigue-Design Hand Book: A Guide for Product Design and Development Engineers," *Advances in Engineering*, Vol. 4, 1968.
- [18] Palmgren, A., "Die Lebensdauer von Kugellagern," *VDI-Zeitschrift*, Vol. 68, 1924, pp. 339–341.
- [19] Miner, M. A., "Cumulative Damage in Fatigue," *Journal of Applied Mechanics*, Vol. 12, 1945, pp. A159–A164.
- [20] Jackson, P., Munson, K., and Taylor, J. W. R., *Jane's All The World's Aircraft*, Jane's Information Group, Surrey, England, U.K., 1995–96.

C. Tan
Associate Editor